Extension to Quadrilateral Element of Three Field Hu-Washizu 2D Elasticity Formulation Based on Biorthogonal Systems

B.P. Lamichhane[1], M.Pingaro[1,*], P.Venini[1,*]

School of Mathematical and Physical Sciences, University of Newcastle, Callaghan, NSW 2308

Department of Civil Engineering and Architecture, University of Pavia, Pavia, Italy

Abstract

New quadrilateral mixed finite element based on modified Hu-Washizu formulation are presented. The stability and consistency of the element are obtained by adding bubble function at the displacement field. Different type of bubble functions are successfully tested. Many examples prove the efficiency and the stability of the element. The extension at the 3D case is straightforward.

Keywords: mixed finite elements, quadrilateral element, Hu-Washizu, biorthogonal systems, elasticity.

1. Introduction

The structure of the papers are the following: first of all in the first section we recall the basic equations of linear elastic problem, in the second section three we briefly recall the modified Hu-Washizu formulations, section four we develop the finite element spaces.

*Corresponding author: Tel. +39 0382 98.5464
Email address: `marco.pingaro@iusspavia.it` (P.Venini)

2. Linear elastic continuum problem

In this section we briefly recovery the equations governing the linear elastic problem. The equilibrium equation is:

$$-\mathrm{div}(\boldsymbol{\sigma}) = \boldsymbol{f} \, , \tag{1}$$

while in small deformation is:

$$\boldsymbol{d} = \boldsymbol{\varepsilon}(\boldsymbol{u}) = \frac{1}{2}(\boldsymbol{\nabla}\, \boldsymbol{u} + \boldsymbol{\nabla}\, \boldsymbol{u}^T) \, . \tag{2}$$

In the case of linear elasticity we have:

$$\boldsymbol{\sigma} = \lambda\, tr(\boldsymbol{\varepsilon})\boldsymbol{I} + 2\mu\, \boldsymbol{\varepsilon} \tag{3}$$

where μ and λ are the Lamé constant. By some algebra one obtains:

$$\boldsymbol{\sigma} = \begin{pmatrix} \lambda(\varepsilon_{11} + \varepsilon_{22}) & 0 \\ 0 & \lambda(\varepsilon_{11} + \varepsilon_{22}) \end{pmatrix} + 2\mu \begin{pmatrix} \varepsilon_{11} & \varepsilon_{12} \\ \varepsilon_{12} & \varepsilon_{22} \end{pmatrix} , \tag{4}$$

and rearranging the equation (4):

$$\boldsymbol{\sigma} = \begin{pmatrix} (\lambda + 2\mu)\varepsilon_{11} + \lambda\, \varepsilon_{22} & 2\mu\, \varepsilon_{12} \\ 2\mu\, \varepsilon_{12} & (\lambda + 2\mu)\, \varepsilon_{22} + \lambda\, \varepsilon_{11} \end{pmatrix} . \tag{5}$$

3. Briefly introduction to modify Hu-Washizu

We define the trial variables: $\boldsymbol{\varepsilon}(\boldsymbol{u})$, $\boldsymbol{d}$ and $\boldsymbol{\sigma}$, while the test variables are: $\boldsymbol{\varepsilon}(\boldsymbol{v})$, $\boldsymbol{e}$ and $\boldsymbol{\tau}$.

$$-\int_\Omega \mathrm{div}(\boldsymbol{C} : \boldsymbol{d})) \cdot \boldsymbol{v} = \boldsymbol{f} \tag{6}$$

$$\begin{aligned} a((\boldsymbol{u}, \boldsymbol{d}), (\boldsymbol{v}, \boldsymbol{e})) + b((\boldsymbol{v}, \boldsymbol{e}), \boldsymbol{\sigma}) &= l(\boldsymbol{v}) && (7) \\ b((\boldsymbol{u}, \boldsymbol{d}), \boldsymbol{\tau}) &= 0 && (8) \end{aligned}$$

where:

$$\begin{aligned} a((\boldsymbol{u}, \boldsymbol{d}), (\boldsymbol{v}, \boldsymbol{e})) &= \int_\Omega \boldsymbol{d} : (\boldsymbol{C} : \boldsymbol{e})\, dx + \alpha \int_\Omega (\boldsymbol{\varepsilon}(\boldsymbol{u}) - \boldsymbol{d}) : (\boldsymbol{\varepsilon}(\boldsymbol{v}) - \boldsymbol{e})\, dx \, , && (9) \\ b((\boldsymbol{u}, \boldsymbol{d}), \boldsymbol{\tau}) &= \int_\Omega (\boldsymbol{\varepsilon}(\boldsymbol{u}) - \boldsymbol{d}) : \boldsymbol{\tau}\, dx \, . && (10) \end{aligned}$$

The modify weak formulation of the problem is:

$$\begin{cases} \alpha \displaystyle\int_\Omega (\boldsymbol{\varepsilon}(\boldsymbol{u}) - \boldsymbol{d}) : \boldsymbol{\varepsilon}(\boldsymbol{v})\, dx + \int_\Omega \boldsymbol{\varepsilon}(\boldsymbol{v}) : \boldsymbol{\sigma}\, dx = \int_\Omega \boldsymbol{f} \cdot \boldsymbol{v}\, dx \\ \displaystyle\int_\Omega \boldsymbol{d} : \boldsymbol{C}\boldsymbol{e}\, dx - \alpha \int_\Omega (\boldsymbol{\varepsilon}(\boldsymbol{u}) - \boldsymbol{d}) : \boldsymbol{e}\, dx - \int_\Omega \boldsymbol{e} : \boldsymbol{\sigma}\, dx = 0 \\ \displaystyle\int_\Omega (\boldsymbol{\varepsilon}(\boldsymbol{u}) - \boldsymbol{d}) : \boldsymbol{\tau}\, dx = 0 \end{cases} \tag{11}$$

by rearranging:

$$\begin{cases} \alpha \int_\Omega \boldsymbol{\varepsilon}(\boldsymbol{u}) : \boldsymbol{\varepsilon}(\boldsymbol{v})\, dx - \alpha \int_\Omega \boldsymbol{d} : \boldsymbol{\varepsilon}(\boldsymbol{v})\, dx + \int_\Omega \boldsymbol{\varepsilon}(\boldsymbol{v}) : \boldsymbol{\sigma}\, dx & = \int_\Omega \boldsymbol{f} \cdot \boldsymbol{v}\, dx \\ -\alpha \int_\Omega \boldsymbol{\varepsilon}(\boldsymbol{u}) : \boldsymbol{e}\, dx + \int_\Omega \boldsymbol{d} : \boldsymbol{C}\boldsymbol{e}\, dx + \alpha \int_\Omega \boldsymbol{d} : \boldsymbol{e}\, dx - \int_\Omega \boldsymbol{e} : \boldsymbol{\sigma}\, dx & = 0 \\ \int_\Omega \boldsymbol{\varepsilon}(\boldsymbol{u}) : \boldsymbol{\tau}\, dx - \int_\Omega \boldsymbol{d} : \boldsymbol{\tau}\, dx & = 0 \end{cases} \tag{12}$$

It is possible to rewrite the system in equation (12) in matrix form in the following way:

$$\begin{bmatrix} \alpha \boldsymbol{A} & -\alpha \boldsymbol{B} & \boldsymbol{W} \\ -\alpha \boldsymbol{B}^T & \boldsymbol{K} + \alpha \boldsymbol{M} & -\boldsymbol{D} \\ \boldsymbol{W}^T & -\boldsymbol{D}^T & \boldsymbol{0} \end{bmatrix} \begin{bmatrix} \boldsymbol{x}_u \\ \boldsymbol{x}_d \\ \boldsymbol{x}_\sigma \end{bmatrix} = \begin{bmatrix} \boldsymbol{b}_f \\ \boldsymbol{0} \\ \boldsymbol{0} \end{bmatrix}, \tag{13}$$

where $\boldsymbol{A} = \int_\Omega \boldsymbol{\varepsilon}(\boldsymbol{u}) : \boldsymbol{\varepsilon}(\boldsymbol{v})$, $\boldsymbol{B} = \int_\Omega \boldsymbol{d} : \boldsymbol{\varepsilon}(\boldsymbol{v})$, $\boldsymbol{W} = \int_\Omega \boldsymbol{\sigma} : \boldsymbol{\varepsilon}(\boldsymbol{v})$, $\boldsymbol{K} = \int_\Omega \boldsymbol{C}\boldsymbol{e} : \boldsymbol{d}$, $\boldsymbol{M} = \int_\Omega \boldsymbol{e} : \boldsymbol{d}$, $\boldsymbol{D} = \int_\Omega \boldsymbol{\sigma} : \boldsymbol{e}$. $\boldsymbol{D}$ is a diagonal matrix. Using this property it is possible condense statically $\boldsymbol{x}_d$ and $\boldsymbol{x}_\sigma$, and we obtain the following system in the only unknown $\boldsymbol{x}_u$:

$$\left[\alpha \boldsymbol{A} - \alpha \left(\boldsymbol{B}\boldsymbol{D}^{-1}\boldsymbol{W}^{-T} + \boldsymbol{W}\boldsymbol{D}^{-1}\boldsymbol{B}^T\right) + \boldsymbol{W}\boldsymbol{D}^{-1}\left(\boldsymbol{K} + \alpha \boldsymbol{M}\right)\boldsymbol{D}^{-1}\boldsymbol{W}^T\right] \boldsymbol{x}_u = \boldsymbol{b}_f \tag{14}$$

4. Finite element discretization

We consider a quasi-uniform triangulation $\mathcal{T}_h$ of the polygonal domain Ω consists of simply, either quadrilateral or hexahedral. We take into account of standard bilinear finite element space $K_h \subset H^1(\Omega)$ defined on the triangulation $\mathcal{T}_h$, where:

$$K_h := \left\{ v \in C^0(\Omega) : v_{|T} \in \mathcal{Q}_1(T),\, T \in \mathcal{T}_h \right\}, \quad K_h^0 = K_h \cap H_0^1(\Omega), \tag{15}$$

and the space of bubble functions

$$B_h := \left\{ b_T \in H^1(T) : b_{T|\partial T} = 0 \text{ and } \int_T b_T \, dx > 0, \; T \in \mathcal{T}_h \right\}, \tag{16}$$

and we define the spaces for strain and displacement as $\boldsymbol{S}_h := [K_h]^{2\times 2}$ and $\boldsymbol{V}_h := [K_h^0 \bigoplus B_h]^2$. In the next section we discuss the different choosing of bubble functions. For the discrete stress space we use:

$$\boldsymbol{M}_h := \left\{ \boldsymbol{\tau}_h \in [M_h]^{2\times 2} : \int_\Omega \boldsymbol{\tau}_h : \mathbf{1} \, dx = 0 \right\} \subset \boldsymbol{S}_0 \,, \tag{17}$$

and let $\{\phi_1, \cdots, \phi_n\}$ and $\{\mu_1, \cdots, \mu_n\}$ the n the basis functions for the space V_h and M_h respectively, we construct the functions μ_i using the following biorthogonality property between the space V_h and M_h:

$$\int_\Omega \mu_i \phi_j \, dx = c_j \delta_{ij} \,, \;\; c_j \neq 0 \,, \;\; 1 \leq i, j \leq n \,, \tag{18}$$

where δ_{ij} is Kronecker symbol, and c_j is a scaling factor which can be chosen to be proportion al to the area of support of ϕ_j. The local basis function of K_h and M_h for the reference square element (see figure 1) $\hat{T} := \{(x, y) : -1 \leq x \leq 1 \,, -1 \leq y \leq 1\}$ are:

$$\begin{aligned} \phi_1 &= \frac{1}{4}(1-x)(1-y) \,, \quad \phi_2 = \frac{1}{4}(1+x)(1-y) \,, \\ \phi_3 &= \frac{1}{4}(1+x)(1+y) \,, \quad \phi_4 = \frac{1}{4}(1-x)(1+y) \,. \end{aligned} \tag{19}$$

and

$$\begin{aligned} \mu_1 &= 1 - 3x - 3y + 9xy \,, \quad \mu_2 = 1 + 3x - 3y - 9xy \,, \\ \mu_3 &= 1 + 3x + 3y + 9xy \,, \quad \mu_4 = 1 - 3x + 3y + 9xy \,. \end{aligned} \tag{20}$$

It is important to observe that the global basis functions of the space M_h are not continuous.

5. Bubble functions

In this section we detail the different choosing of the bubble functions. Addition of the bubble functions is essential to create a stable space. we have four types of bubbles. In the first two cases we use a modification of the standard bubble function ,that is for the reference element:

$$b_T(x, y) = (1 - x^2)(1 - y^2) \,, \tag{21}$$

while in the next two, we add to the standard bubble function another one.

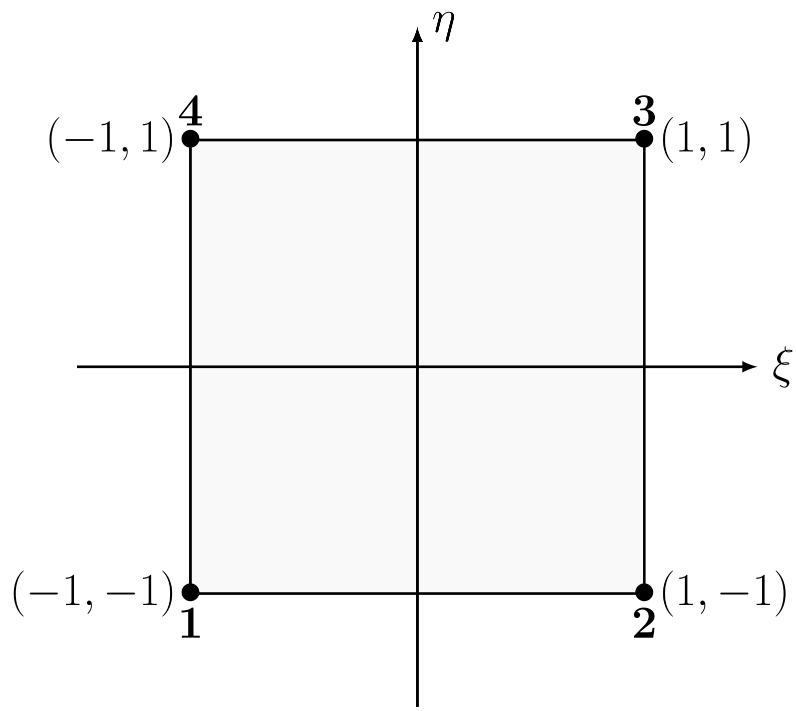

Figure 1: Reference Element

5.1. One Bubble function (type 1)

As a first choice of bubble function we use:

$$\hat{b}_T(x,y) = c_T \cdot \phi_T(x,y) \cdot b_T(x,y)\ , \tag{22}$$

where c_T is a coefficient in order to obtain $\hat{b}_T(x_g,y_g) = 1$ (where $\boldsymbol{g}$ is the centroid of the elements), ϕ_K is the standard bilinear basis function corresponding to the lower-left corner of the square T. In the case of reference square element we obtain:

$$\hat{b}_T(x,y) = (1-x)(1-y)(1-x^2)(1-y^2)\ . \tag{23}$$

5.2. One Bubble function (type 2)

The second choice of bubble function we take:

$$\hat{b}_T(x,y) = c_T \cdot (a + bx + cy) \cdot b_T(x,y)\ , \tag{24}$$

where $a, b, c \in \mathrm{R}$ and $a, b, c \neq 0$. For simplicity we set $a = b = c = 1$ and we obtain for the reference square:

$$\hat{b}_T(x, y) = (1 + x + y)(1 - x^2)(1 - y^2)\;. \tag{25}$$

5.3. Two Bubble functions

Using two bubble functions, where the first is the standard bubble function and the second bubble is a modification of the standard bubble:

$$\begin{aligned} \hat{b}_{T1}(x, y) &= b_T\;, \\ \hat{b}_{T2}(x, y) &= c_T \cdot (ax + by) \cdot b_T\;, \end{aligned} \tag{26}$$

where $a, b \in \mathrm{R}$ and $a^2 + b^2 \neq 0$. For the sake of simplicity we adopt $a = b = 1$. One obtains:

$$\begin{aligned} \hat{b}_{T1}(x, y) &= (1 - x^2)(1 - y^2)\;, \\ \hat{b}_{T2}(x, y) &= (x + y)(1 - x^2)(1 - y^2)\;. \end{aligned} \tag{27}$$

5.4. Two Bubble functions, which one mixed

As a finally choice of bubbles we use a standard bubble function plus one mixed bubble function for the two components of displacement.

$$\begin{aligned} \hat{b}_{T1}(x, y) &= b_T\;, \\ \hat{b}_{T2,x}(x, y) &= (\nabla\phi_1)_x \cdot b_T\;, \\ \hat{b}_{T2,y}(x, y) &= (\nabla\phi_1)_y \cdot b_T\;, \end{aligned} \tag{28}$$

where $(\nabla\phi_1)_i$ is i-th component of the gradient of the first shape function ϕ. In this way we have as shape function for the displacement using the mixed bubble function the vector $\left[\hat{b}_{T2,x}(x, y), \hat{b}_{T2,y}(x, y)\right]$.

6. Numerical example

In this section we report some examples using the presented formulation to proven the good behaviour.

6.1. *Square problem*

First example is a unit square domain with homogeneous Dirichlet boundary conditions. The Lamé constant are fix to $\lambda = 123$ and $\mu = 79.3$. By imposition of the previously exact solution one obtain for the body force f

$$
\begin{aligned}
f_1 &= -\pi^2 \cos(\pi x) \sin(\pi y) \left(\lambda + \mu + 2\lambda \cos(\pi y) + 12\mu \cos(\pi y)\right), \\
f_2 &= -\pi^2 \sin(\pi x) \big(\lambda \cos(\pi y) + 3\mu \cos(\pi y) + 2\lambda \left(2\cos(\pi y)^2 - 1\right) \\
&\quad +2\mu \left(2\cos(\pi y)^2 - 1\right)\big)
\end{aligned} \tag{29}
$$

The exact solution is

$$
u_1 = \cos(\pi x) \sin(2\pi y), \;\; u_2 = \sin(\pi x) \cos(\pi y). \tag{30}
$$

The problem is study using two type of mesh: first of all using a square mesh and before using a trapezoidal mesh. The two types of mesh are shown in figures 2(a) and 2(b). Figures 3(a), 3(b), 4(a) and 4(b) shown the error in norm L^2 in the case of regular mesh for the different types of bubble functions used and types of coefficient α. All types of element converge in a good way. In Figures 5(a), 5(b), 6(a) and 6(b) we report the previously results in the case of trapezoidal meshes.

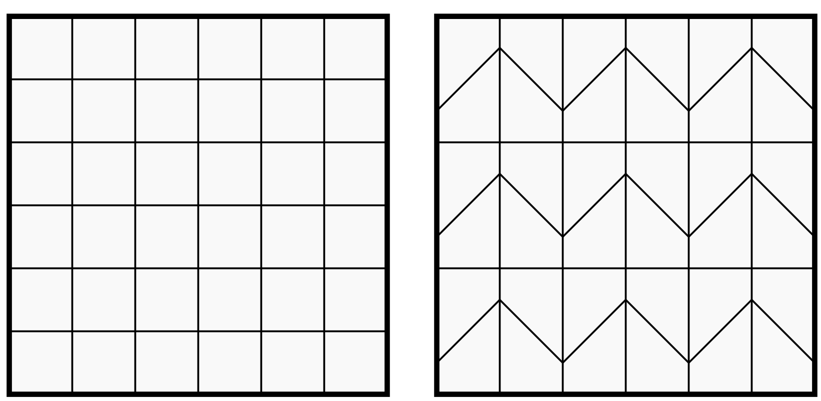

(a) Regular mesh (b) Trapezoidal mesh

Figure 2: Square Problem

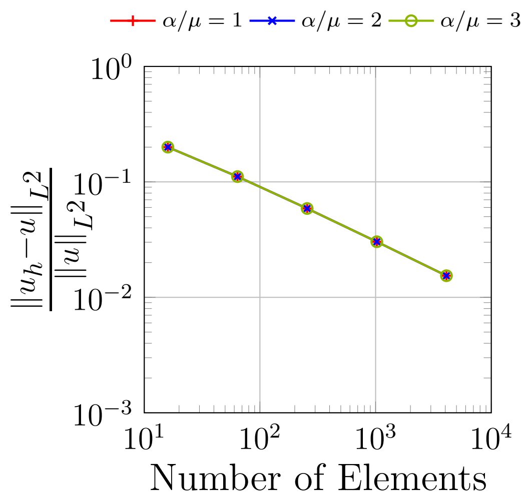

(a) type 1

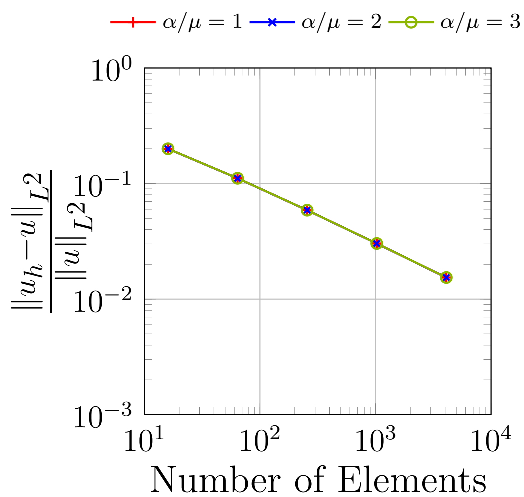

(b) type 2

Figure 3: The relative error vs. the number of elements measured relative to the L^2 norm (Case one bubble function and regular mesh)

6.2. Cantilever beam problem

Now we consider the beam with length $L = 10$ and height $l = 2$ as we shown in figure (). The Young modulus is set equal to $E = 1500$ and the Poisson $\nu = 0.4999$ and subjected to a distributed load as in figure 7 with

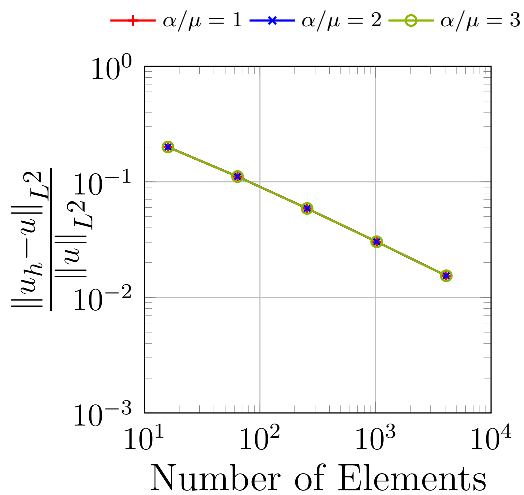

(a) Case two bubble function

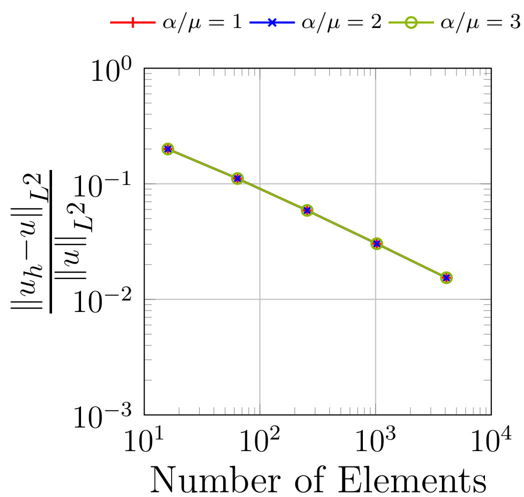

(b) Case two bubble function of which one mixed

Figure 4: The relative error versus the number of elements measured relative to the L^2 norm (regular mesh)

$f = 300$. The exact solution is:

$$
\begin{aligned}
u(x,y) &= \frac{2f}{El}(1-\nu^2)x\left(\frac{l}{2}-y\right) , \\
v(x,y) &= \frac{f}{El}\left[x^2 + \frac{\nu}{1-\nu}\left(y^2 - ly\right)\right] .
\end{aligned}
\tag{31}
$$

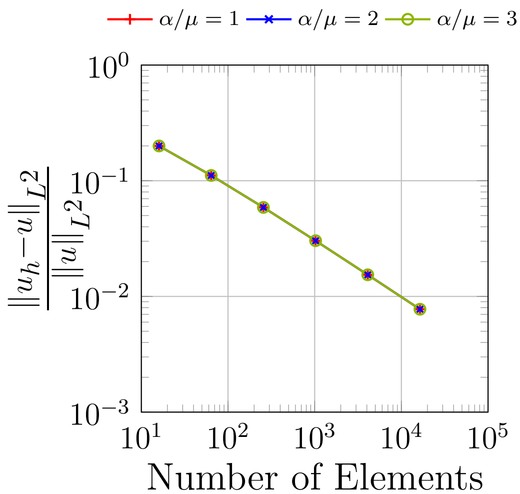

(a) type 1

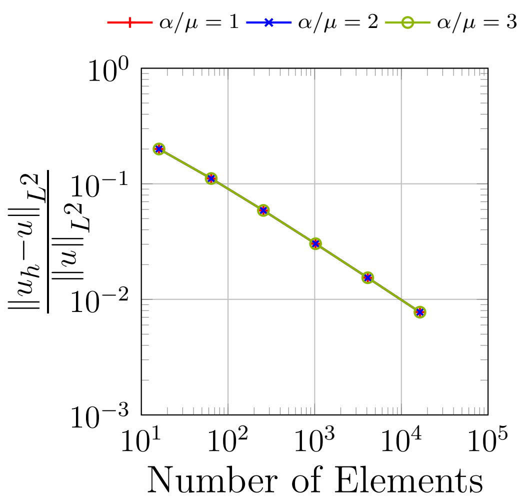

(b) type 2

Figure 5: The relative error vs. the number of elements measured relative to the L^2 norm (Case one bubble function and Trapezoidal mesh)

We use to model the beam two types of mesh: regular anf trapezoidal as in the previously example (see figures 2(a) and 2(b)). we shown in figures 10(a), 10(b), 11(a) and 11(b) the L^2-norm error for different types of bubble functions used in the case of $\alpha/mu := 1, 2, 3$, while in figures 10(a), 10(b),

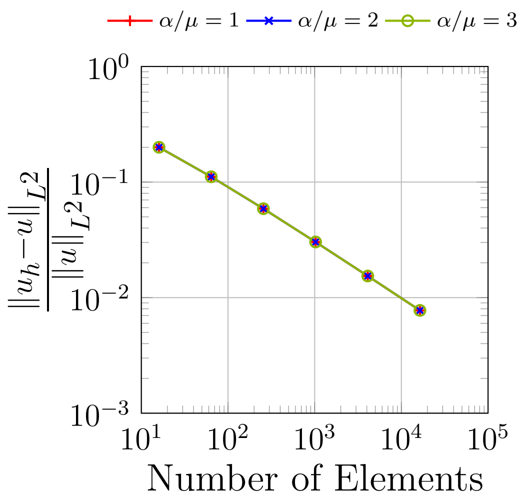

(a) Case two bubble function

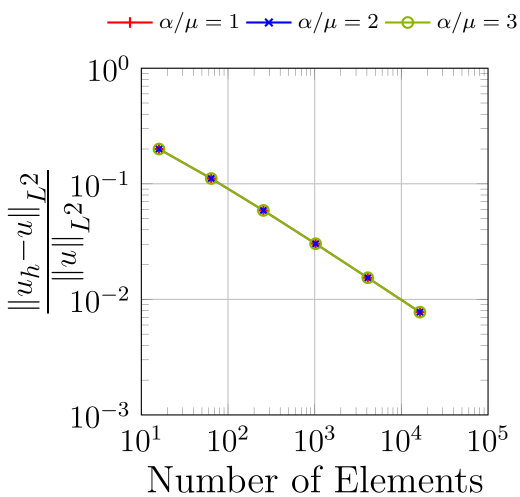

(b) Case two bubble function of which one mixed

Figure 6: The relative error vs. the number of elements measured relative to the L^2 norm (Case one bubble function and Trapezoidal mesh)

11(a) and 11(b) the same plots using trapezoidal meshes. In the all cases the elements distorted have a good behaviour respect to the regular mesh.

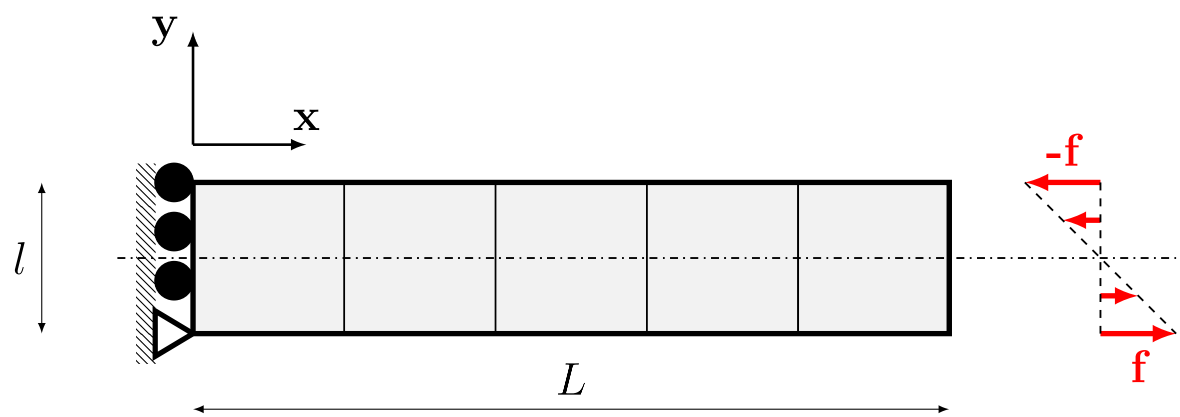

Figure 7: Beam cantilever geometry

6.3. *Cook's membrane*

The final example is the Cook's membrane. That is a typical benchmark and consist of a beam with vertex: $(0,0)$, $(48,44)$, $(48,60)$ and $(0,44)$. The left vertical edge is clamped and the right vertical edge subjected to the vertical distributed forces with resultant $F = 100$ as it shown in figure 12. The material properties are taken to be $E = 250$ and $\nu = 0.4999$, so that a nearly incompressible response is obtained. We report in figures 13(a), 13(b), 13(c) and 13(d) the vertical displacement of the point A versus the number of element per side for different choosing of the parameter $\alpha = \{1, \mu, 2\mu, 3\mu\}$. All elements return different behaviour using different coefficients α. In the case of $\alpha = 1$, figure 13(a), the obtained results completely not converge to the reference solution.

7. Conclusions

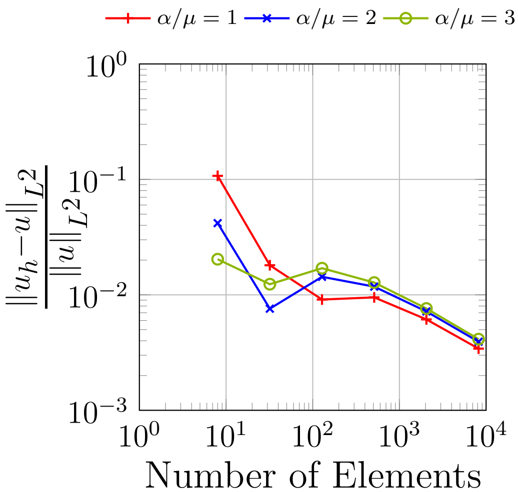

(a) Type 1

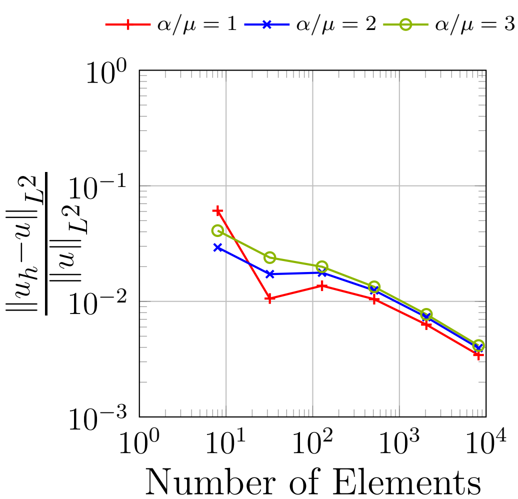

(b) Type 2

Figure 8: Beam Cantilever: the relative error vs. the number of elements measured relative to the L^2 norm (regular mesh)

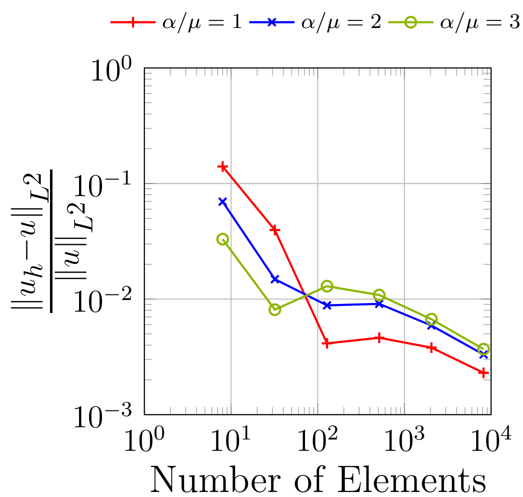

(a) Case two bubble function

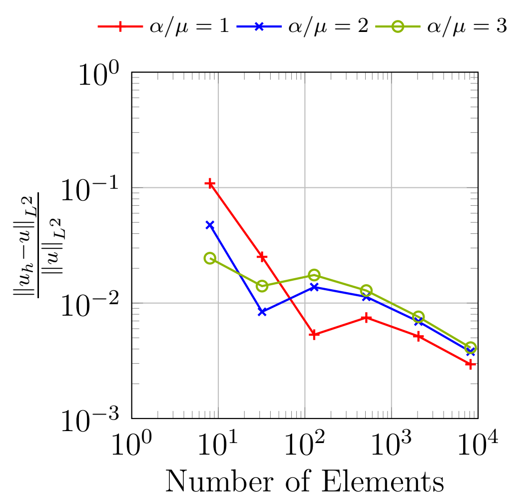

(b) Case two bubble function of which one mixed

Figure 9: Beam Cantilever: the relative error vs. the number of elements measured relative to the L^2 norm (regular mesh)

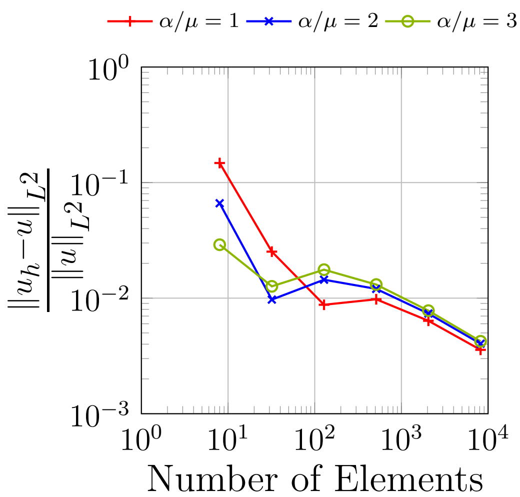

(a) Type 1

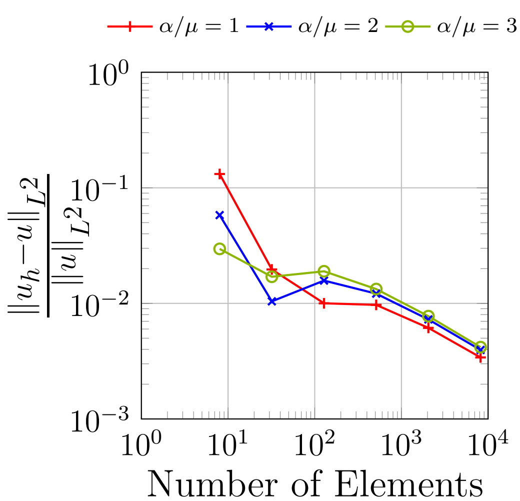

(b) Type 2

Figure 10: Beam Cantilever: the relative error vs. the number of elements measured relative to the L^2 norm (trapezoidal mesh)

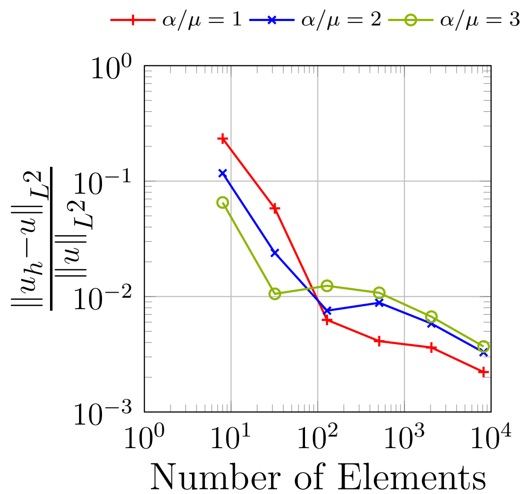

(a) Case two bubble function

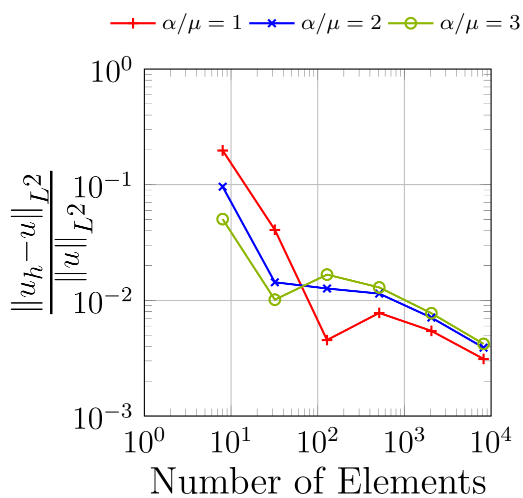

(b) Case two bubble function of which one mixed

Figure 11: Beam Cantilever: the relative error vs. the number of elements measured relative to the L^2 norm (trapezoidal mesh)

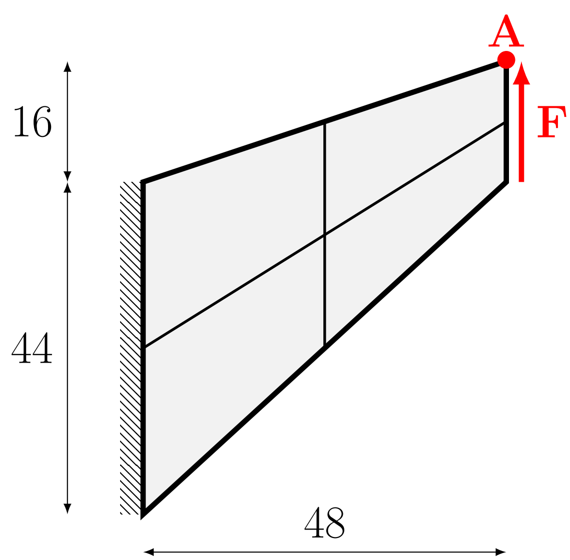

Figure 12: Cook's Membrane geometry

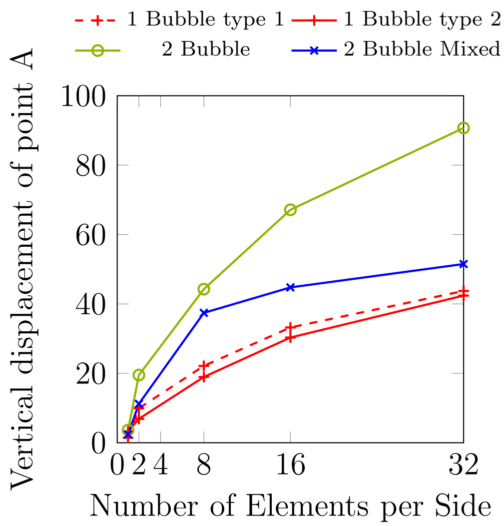

(a) $\alpha = 1$

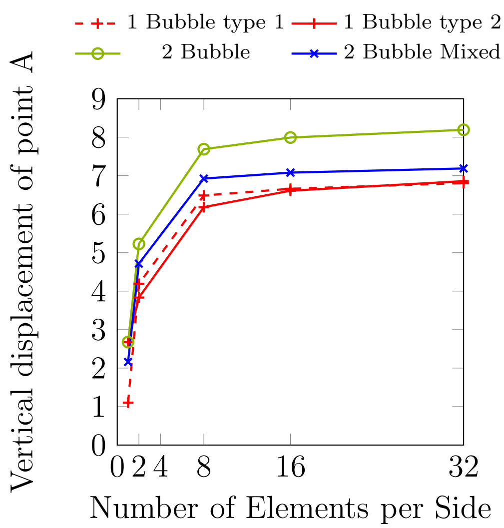

(b) $\alpha/\mu = 1$

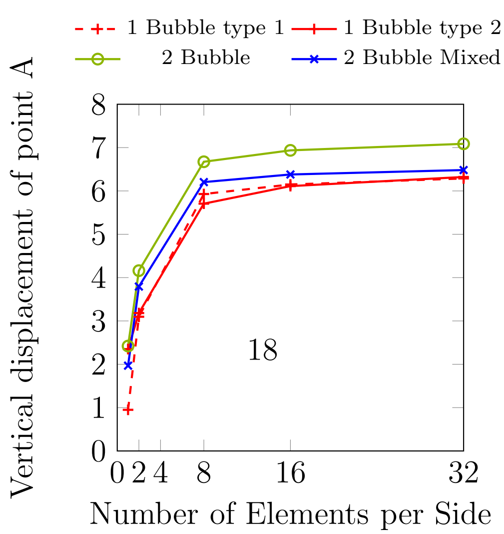

(c) $\alpha/\mu = 2$